JOURNAL OF MATERIALS SCIENCE 33 (1998) 5277–5289

# Chemical, mechanical and microstructural characterization of low-oxygen containing silicon carbide fibers with ceramic coatings

N. P. BANSAL
*National Aeronautics and Space Administration, Lewis Research Center, Cleveland, OH 44135, USA*
*E-mail: narottam.p.bansal@lerc.nasa.gov*

Y. L. CHEN
*Dynacs, Inc., Lewis Research Center Group, Brookpark, OH 44142, USA*

Room temperature tensile strengths of as-received Hi-Nicalon fibers and those having BN/SiC, p-BN/SiC, and p-B(Si)N/SiC surface coatings, deposited by chemical vapor deposition, were measured using an average fiber diameter of 13.5 $\mu$m. The Weibull statistical parameters were determined for each fiber. The average tensile strength of uncoated Hi-Nicalon was $3.19 \pm 0.73$ GPa with a Weibull modulus of 5.41. Strength of fibers coated with BN/SiC did not change. However, fibers coated with p-BN/SiC and p-B(Si)N/SiC surface layers showed strength loss of $\sim$10% and 35%, respectively, compared with the as-received fibers.

The elemental compositions of the fibers and the coatings were analyzed using scanning Auger microprobe and energy dispersive X-ray spectroscopy. The BN coating was contaminated with a large concentration of carbon and some oxygen. In contrast, p-BN, p-B(Si)N, and SiC coatings did not show any contamination. Microstructural analyses of the fibers and the coatings were done by scanning electron microscopy (SEM), transmission electron microscopy (TEM), and selected area electron diffraction. Hi-Nicalon fiber consists of fine $\beta$-SiC nanocrystals ranging in size from 1 to 30 nm embedded in an amorphous matrix. TEM analysis of the BN coating revealed four distinct layers with turbostratic structure. The p-BN layer was turbostratic and showed considerable preferred orientation. The p-B(Si)N was glassy and the silicon and boron were uniformly distributed. The silicon carbide coating was polycrystalline with a columnar structure along the growth direction. The p-B(Si)N/SiC coatings were more uniform, less defective and of better quality than the BN/SiC or the p-BN/SiC coatings. 

## 1. Introduction

Polymer derived, small diameter Hi-Nicalon silicon carbide fibers [1], because of their high strength and excellent strength retention after high temperature exposures, are currently of great technical interest as a reinforcement in high performance structural composites with polymer, metal, and ceramic matrices. However, these fibers need to be protected against chemical reactions with metal and ceramic matrices during composite processing and use, and also against oxidizing and other harsh environments. The protective ceramic surface coating(s) on the fiber surface also provide a weak fiber/matrix interface [2–3] for toughened ceramic matrix composites. The BN/SiC dual layer is the state-of-the-art interface coating for ceramic matrix composites. The pyrolytic boron nitride (p-BN) coating is more stable than BN. Also, silicon containing pyrolytic boron nitride (p-B(Si)N) shows [4] 1–3 orders of magnitude greater oxidation resistance at elevated temperatures than p-BN and is more resistant to reaction with moisture. It is necessary to know if the application of these coatings results in any strength degradation or microstructural changes in Hi-Nicalon fibers.

The primary objective of the present study was to investigate the effects of various BN/SiC type surface coatings on the tensile strength of Hi-Nicalon fibers. Another objective was to carry out chemical and microstructural analyses of the fibers and the coatings. Microstructural analyses of the fiber and the coatings were done by scanning electron microscopy (SEM) and transmission electron microscopy (TEM). Elemental compositions and thicknesses of the fiber and the coatings were determined by scanning Auger microprobe, energy dispersive analysis of X-rays (EDAX), and electron microscopy. Room temperature tensile strength was measured and the Weibull statistical parameters were determined for fibers with different coatings.

TABLE I Properties of Hi-Nicalon fibers*

| Property | Value |
|---|---|
| Density (g/cm$^3$) | 2.74 |
| Diameter ($\mu$m) | 14 |
| Filaments/tow | 500 |
| Denier (g/9000 m) | 1800 |
| Tensile strength (GPa) | 2.8 |
| Elastic modulus (GPa) | 269 |
| Thermal expansion coefficient ($10^{-6}$/K) | 3.5 (25–500 °C) |
| Specific heat (J/g-K) | 0.67 (25 °C) |
| | 1.17 (500 °C) |
| Thermal conductivity (W/m-K) | 7.77 (25 °C) |
| | 10.1 (500 °C) |
| Electrical resistivity (ohm-cm) | 1.4 |
| Chemical composition (wt %) | 63.7 Si, 35.8 C, 0.5 O |
| C/Si, atomic ratio | 1.3–1.4 |
| Temperature capability (°C) | 1200 |

*Data from Nippon Carbon Co.

## 2. Materials

Hi-Nicalon fiber from Nippon Carbon Co. was used in the present study. The properties of the as-received fiber are shown in Table I. These fibers consist of $\beta$-SiC, a small amount of silicon oxycarbide (<1 wt %), and 30–40 at % excess carbon which is also reflected in its low elastic modulus. A large variation (10–18 $\mu$m) in the fiber diameter was observed, although the manufacturer reports an average value of ~14 $\mu$m.

The polyvinyl alcohol (PVA) sizing on the as-received Hi-Nicalon fibers was burned off in a Bunsen burner flame. Single filaments were carefully separated from the fiber tow for testing. All the coatings on the fibers were applied using a continuous chemical vapor deposition (CVD) reactor by two different vendors. The BN coating ~0.4 $\mu$m thick was deposited by 3M at ~1000 °C utilizing a proprietary precursor. About 0.3 $\mu$m thick overcoating of SiC was also applied to the BN-coated fibers. On the other hand, Advanced Ceramics Corporation deposited p-BN or p-B(Si)N coatings at ~1400 °C using $BCl_3$, $NH_3$, and $SiHCl_3$ as the precursor gases where the yarn residence time in the deposition hot zone was ~1.1 min. An overlayer of SiC was further deposited by CVD. The nominal coating thicknesses were 0.6 $\mu$m of p-BN or p-B(Si)N and 0.3 $\mu$m of SiC.

## 3. Experimental

### 3.1. Electron microscopy

Surfaces of the fibers were examined using SEM and TEM. For cross-sectional analysis, fibers were mounted in a high temperature epoxy and polished before examination. Fiber cross-sectional thin foils for TEM were prepared using a procedure developed for ceramic fibers which involved epoxy potting, slicing, polishing, and argon ion beam milling. A thin carbon coating was evaporated onto the TEM thin foils and SEM specimens for electrical conductivity prior to analysis. The thin foils were examined in a Philips EM400T operating at 120 keV. SEM was performed using a JEOL JSM-840A operating at 15 keV. X-ray elemental analyses were done using a Kevex thin window energy dispersive spectrometer and analyzer.

### 3.2. Scanning Auger analysis

The elemental compositions of the fiber near the surface and of the fiber surface coatings were analyzed [5] with a scanning Auger microprobe (Fisons Instruments Microlab Model 310-F). The fibers for this analysis were mounted on a stainless steel sample mount by tacking the ends with colloidal graphite. Depth profiling was performed by sequential ion-beam sputtering and Auger analysis. The ion etching was done with 3 keV Argon ions rastered over an approximately 1 mm$^2$ area on the specimen. The etch rate in $Ta_2O_5$ under these conditions was 0.05 nm/s.

Auger electron spectroscopy (AES) analysis was performed using an electron beam current of approximately 1.5 nA. The beam was rastered over a $2 \times 20$ $\mu$m$^2$ area of the fiber with the long axis of the area aligned with the long axis of the fiber. Spectra were acquired in integral (as opposed to derivative) form at a beam energy of 2 keV and depth profiles were created by plotting peak areas against ion etch time. The atomic concentrations were calculated by dividing the peak areas by the spectrometer transmission function and the sensitivity factors for each peak, then scaling the results to total 100%. The sensitivity factors were derived from spectra of ion etched Ag, Si, B, Ti, SiC, BN, and $TiO_2$ standards. The sensitivity factors used for each element were accurate to about ±20%. The depth scale is from the $Ta_2O_5$ calibration and no attempt has been made to adjust for the actual etch rate for each material. Only the fibers with a smooth surface coating, rather than those having thick and rough coating morphologies, were used for Auger analysis.

### 3.3. Tensile strength measurements

Room temperature tensile strengths of the individual filaments were measured in ambient atmosphere with a screw driven Micropull fiber test frame equipped with pneumatic grips. A 1000 g load cell, Sensotec model 34, was used. Measurements were carried out at a constant crosshead speed of 1.261 mm/min (0.05 inch/min). A single filament was mounted on a paper tab using Hardman extra fast setting epoxy. The side portions of the tab were cut with a hot wire just before application of the load producing a fiber gage length of 2.54 cm (1 inch). Twenty filaments of each type of fiber were tested. Weibull parameters for tensile strength of fibers were calculated based on an average fiber diameter of 13.5 $\mu$m.

## 4. Results and discussion

### 4.1. Electron microscopic analysis

#### *4.1.1. Hi-Nicalon fiber*

SEM micrographs showing the surface of as-received, flame desized Hi-Nicalon fibers are presented in Fig. 1. The fiber surface appears to be fairly smooth and featureless. EDS compositional spectra (Fig. 2) taken from the polished cross-section of the fiber indicate the presence of only Si and C along with a small amount of oxygen which is in qualitative agreement with the manufacturer's data (Table I). A pair of TEM bright-field (a) and dark-field (b) images from Hi-Nicalon fiber along with

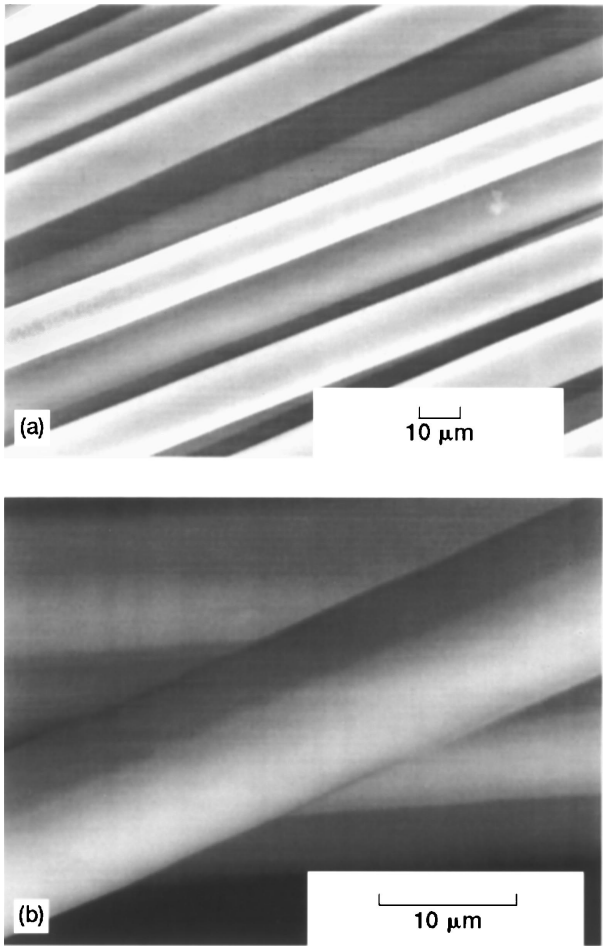


*Figure 1* SEM micrographs showing surface of desized Hi-Nicalon fibers.

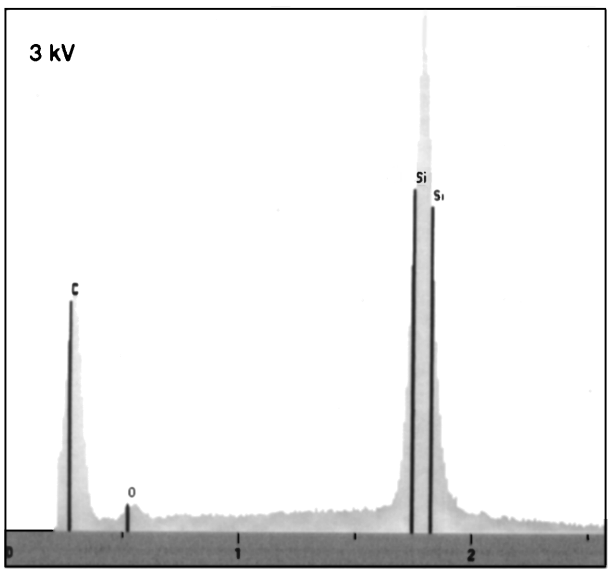


*Figure 2* EDS spectra from the cross-section of desized Hi-Nicalon fiber at 3 kV.

the selected-area diffraction pattern (SADP) shown as the inset are given in Fig. 3. These results indicate that Hi-Nicalon fiber consists of a SiC nanocrystalline structure, i.e., fine $\beta$-SiC crystallites (white features in dark-field) of size ranging from 1 to 30 nm which are imbedded in an amorphous matrix, probably carbon. The apparent mean grain size of the $\beta$-SiC crystallites

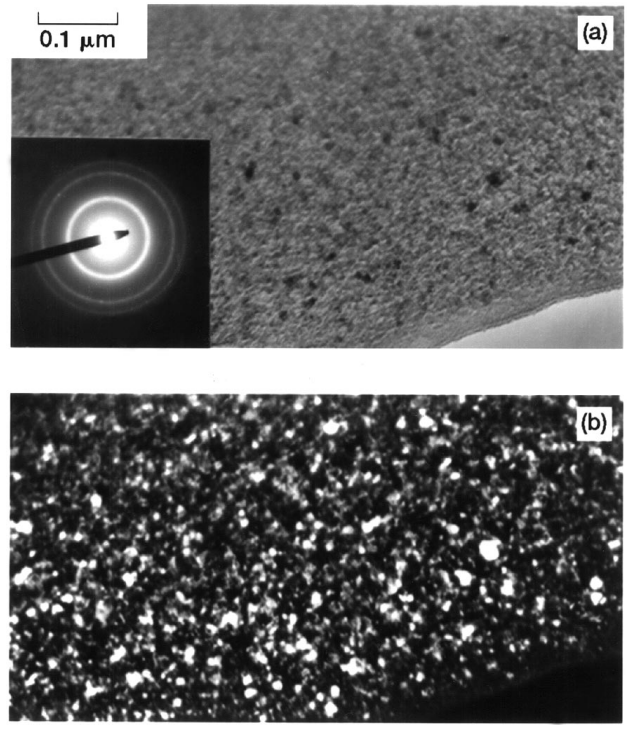


*Figure 3* Pair of TEM bright-field (a) and dark-field (b) images from desized Hi-Nicalon fiber. The SADP is shown as inset.

calculated from the width of the (1 1 1) X-ray diffraction peak at mid-height using the Scherrer equation has been reported [6, 7] to be about 3–5 nm. No peak assigned to turbostratic carbon was observed [6] in the X-ray diffraction.

### 4.1.2. Hi-Nicalon/BN/SiC fiber

SEM micrographs from the surface and polished cross-section of the BN/SiC coated Hi-Nicalon fibers are given in Fig. 4a and b, respectively. The coating on most of the fibers is smooth and uniform, but some fibers have a quite granular coating. The BN coating is often nodular as can be seen in Fig. 5a. The nodules in the BN layer remain or, often, are enhanced by the subsequent overcoating of SiC. The number density of the nodules varies considerably from filament to filament, but is more consistent along an individual fiber. Within a tow, the fibers on the outside had thicker and more granular coatings than those on the inside. Overall, the coating thickness was reasonably uniform. Generally, the BN coating thickness was 0.2–0.4 $\mu$m, but could be much higher at the nodules. The total coating thickness on a fiber could be as high as 7 $\mu$m when a granular cluster is attached (Fig. 5a). Typically, the SiC coating thickness varied between 0.2 and 0.3 $\mu$m. Sharp contrast is observed between the fiber, BN coating, and SiC coating in polished cross-sections (Fig. 5b). The microstructure of these coatings is quite similar to those of BN/SiC coatings on HPZ ceramic fibers [5]. TEM analysis of the loose, BN/SiC coated Hi-Nicalon fibers in cross-section revealed four distinct layers in the BN coating (Fig. 6). While there was no detectable variation in composition between the layers, there was a subtle variation in crystallographic structure. All four layers were turbostratic in structure, but layers 1 and 3 (counting from the fiber

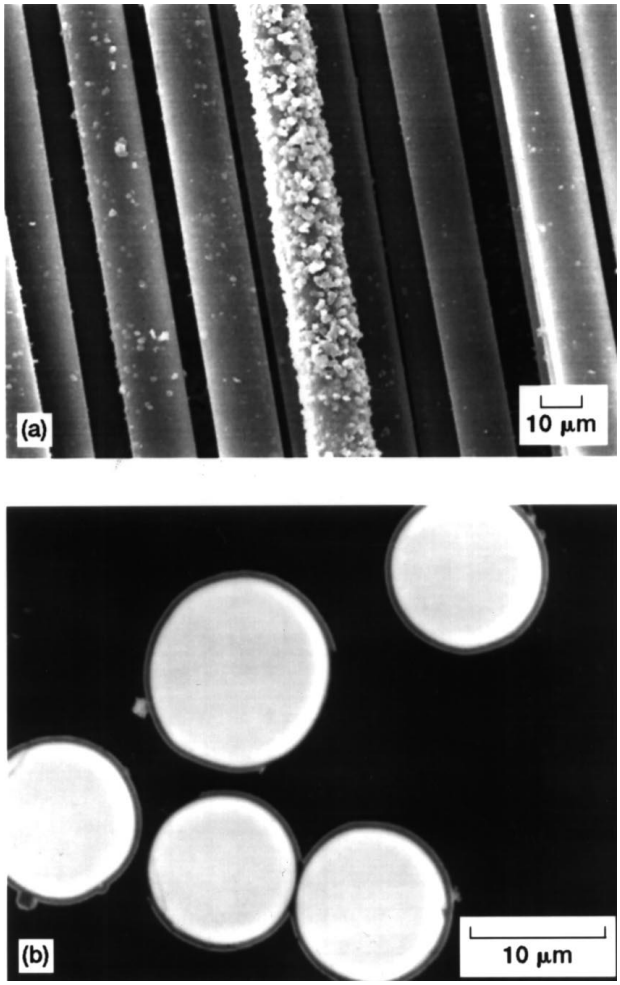


*Figure 4* SEM micrographs from (a) surface and (b) polished cross-section of BN/SiC coated Hi-Nicalon fibers.

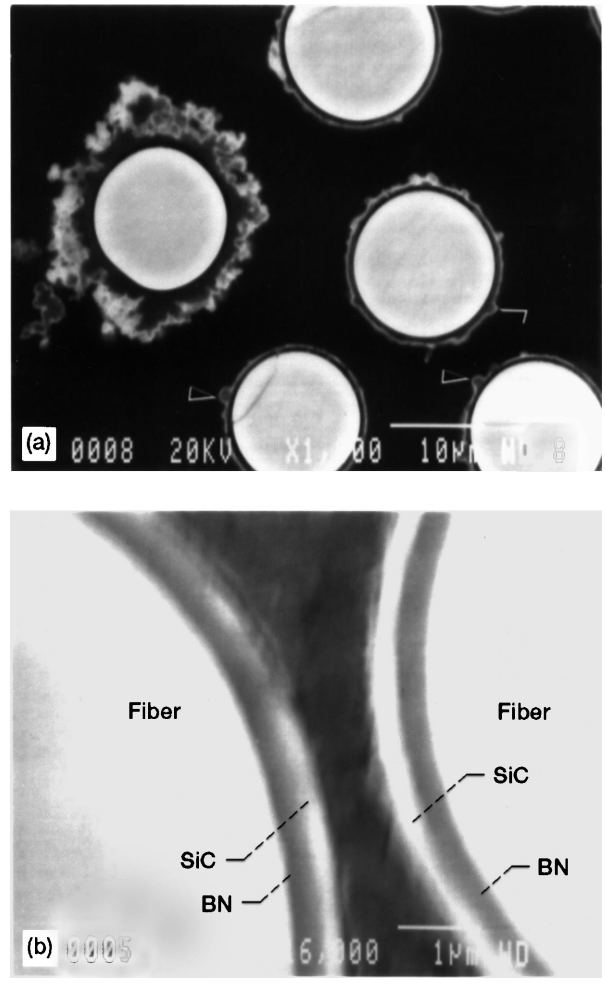


*Figure 5* SEM micrographs from polished cross-sections of BN/SiC coated Hi-Nicalon fibers (a) showing nodular coating; some of the nodules are indicated by arrows and (b) showing sharp contrast between the fiber and the coatings.

outward) were more directional. The basic structural units of the BN are more aligned parallel to the fiber surface, giving sharper cusps in microelectron diffraction patterns (Fig. 6b and c). The SiC layer on the as-coated fibers typically ion milled away before electron transparent thin regions were obtained; but when retained, appeared to be adherent to the BN layers.

### 4.1.3. Hi-Nicalon/p-BN/SiC fiber

SEM micrographs showing polished cross-sections and surfaces of p-BN/SiC coated Hi-Nicalon fibers are given in Figs 7 and 8, respectively. The fiber diameter varies from 10 to 20 $\mu$m with an average diameter of $\sim$13.5 $\mu$m. The coatings are mostly smooth and uniform. However, granular and defective coatings are seen on the surface of some filaments. Nodules in the p-BN layer are seen on some of the fibers which are further enhanced by the SiC overcoating. The number density of these nodules is much lower than in the BN/SiC coating as seen in Figs 4 and 5. Cracks (shown by arrows) are also present in the outer SiC coating on some fibers. Thickness of the p-BN coating ranged from 0.5 to 1.5 $\mu$m, while the SiC coating thickness varied from 0.1 to 0.4 $\mu$m. The arrows in the TEM bright-field image (Fig. 9) from the p-BN/SiC coated fiber indicate the interfaces between the SiC coating and the p-BN coating and between the p-BN coating and the fiber, respectively. There is a darker contrast band in the p-BN coating, probably due to variation in boron and nitrogen concentration. The microstructures of the coatings, the fiber and their interfaces indicated by the arrows in TEM bright-field images in Fig. 10a and b show that: (1) the interface between p-BN coating and SiC coating exhibit a sharp and abrupt transition (Fig. 10a), and the SiC coating is a columnar-like poly-crystalline structure as shown in the selected-area diffraction pattern (SADP) (inset marked SiC), and the direction of the column is along the growth direction; (2) the p-BN coating is typically a layer amorphous phase as shown in SADP (inset marked BN), and a light contrast band is observed between the fiber and the p-BN coating; and (3) the fiber has a SiC nanocrystalline structure, i.e., fine $\beta$-SiC nanocrystals are imbedded in an amorphous matrix as shown in SADP (inset marked fiber). The energy dispersive X-ray spectra (EDXS) from the fiber/p-BN interface, middle of p-BN coating, and SiC coating regions are shown in Fig. 11. Small amount of Si detected in the p-BN coating may be due to interference from the adjoining areas as no Si contamination was observed in the p-BN layer from Auger analysis (see Fig. 18c). The p-BN coating, deposited under

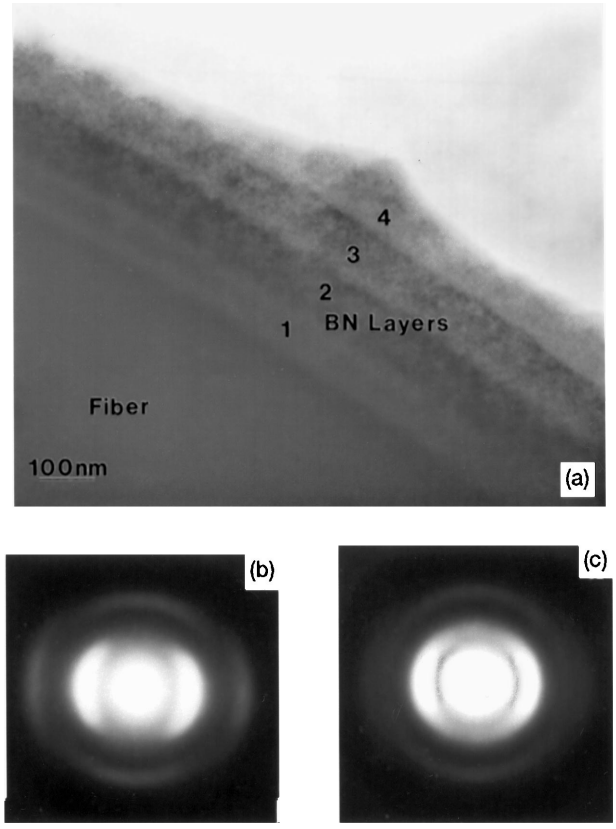


*Figure 6* (a) TEM bright field image showing cross-section of the as-received BN/SiC coated Hi-Nicalon fiber; four distinct sub-layers are visible within the BN coating. Also shown are the microelectron diffraction patterns typical for BN layers: (b) layers 1 and 3 and (c) layers 2 and 4.

conditions similar to the present study, was recently reported [4] to be turbostratic with a rocking curve full-width at half maximum (FWHM) of 70° for the (0 0 2) reflection. Typical crystallite size was 35 Å and the average interlayer spacing ($c_0/2$) was 3.44 Å compared with 3.33 Å for ideal hexagonal BN.

### 4.1.4. Hi-Nicalon/p-B(Si)N/SiC fiber

SEM micrographs showing polished cross-sections and surfaces of p-B(Si)N/SiC coated Hi-Nicalon fibers are given in Figs 12 and 13, respectively. In general, the p-B(Si)N/SiC coatings are more uniform, less defective and of better quality than the p-BN/SiC coatings. The B(Si)N is less nodular and SiC layer is more uniform than p-BN/SiC coatings. The thickness of the p-B(Si)N and SiC coatings varied from 0.5 to 1.5 $\mu$m, and 0.2 to 1.0 $\mu$m respectively.

The TEM dark-field image (Fig. 14) shows the interfaces between SiC coating and p-B(Si)N coating (marked by top arrow), and between the p-B(Si)N coating and the fiber (marked by bottom arrow). The microstructures of the fiber and coatings are characterized by electron diffraction. The SADP from the fiber (inset marked fiber) shows a typical microcrystalline phase. The microdiffraction of p-B(Si)N coating (inset marked BN) reveals that the amorphous layer structure is weaker than that of p-BN. The SiC coating has a columnar-like poly-crystalline structure as shown

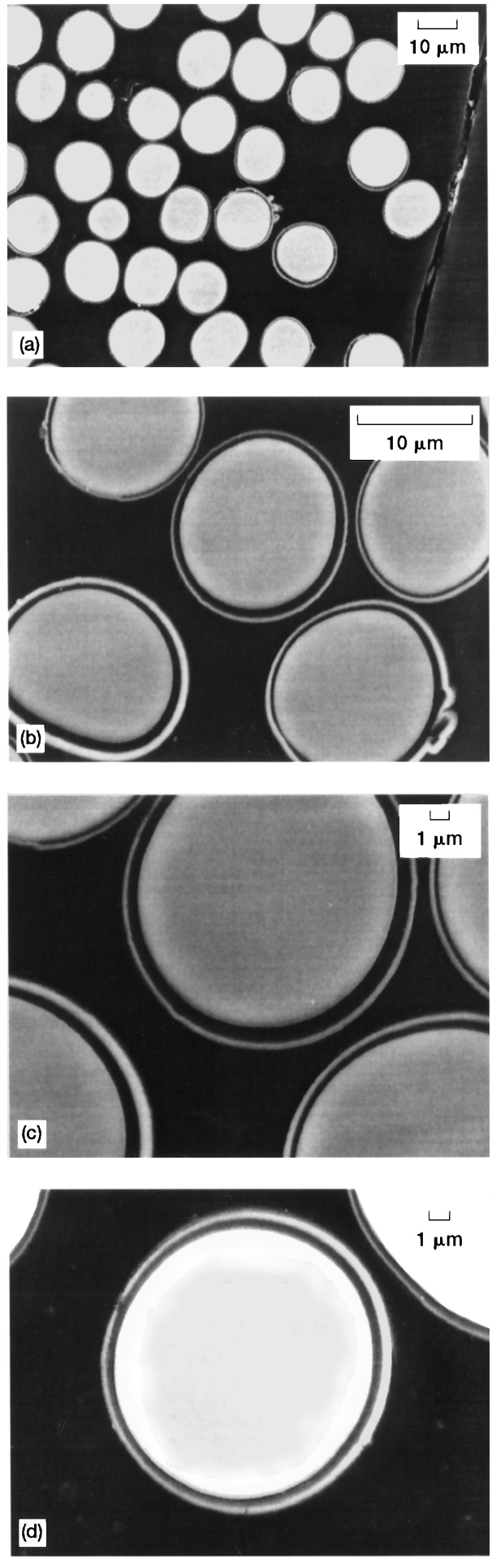


*Figure 7* SEM micrographs showing polished cross-sections of p-BN/SiC coated Hi-Nicalon fibers.

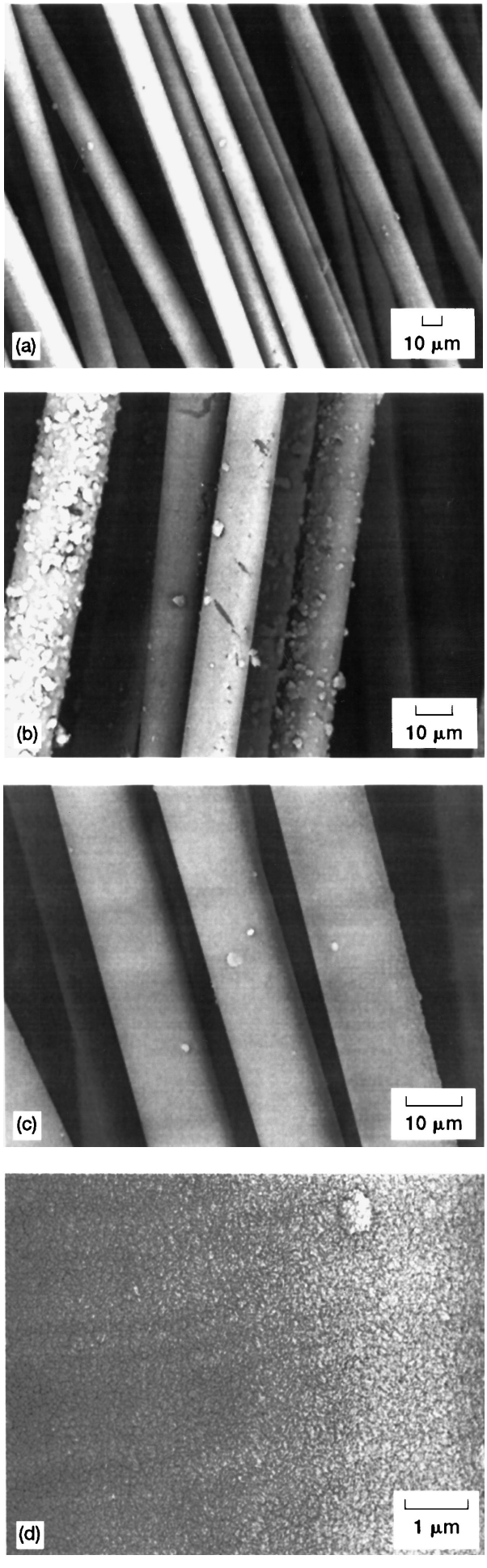


*Figure 8* SEM micrographs showing surfaces of p-BN/SiC coated Hi-Nicalon fibers.

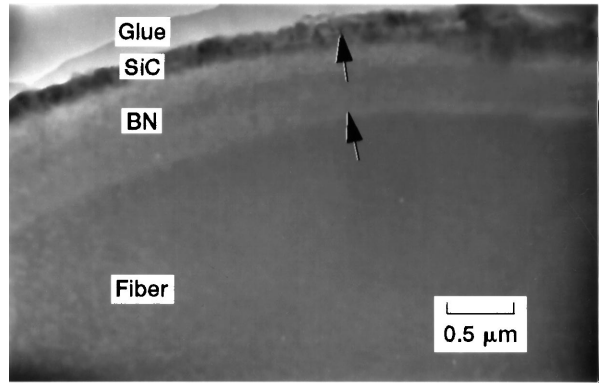


*Figure 9* TEM bright-field image showing interfaces between p-BN and SiC coatings and between fiber and p-BN coating for p-BN/SiC coated Hi-Nicalon fiber.

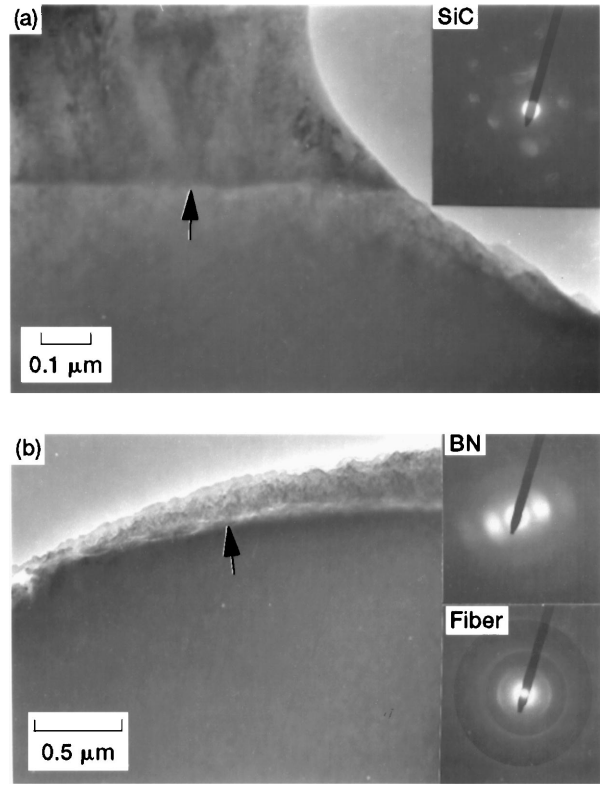


*Figure 10* TEM bright-field images showing microstructures of fiber, coatings and their interfaces for p-BN/SiC coated Hi-Nicalon fiber. Selected area diffraction patterns from the fiber and the p-BN and SiC coatings are shown as insets.

in SADP (inset marked SiC), and the direction of the column is along the growth direction. Some very fine crystallites are present in the p-(B(Si)N coating near the fiber. A higher magnification pair of TEM bright-field/dark-field images (Fig. 15) from the fiber reveals the presence of $\beta$-SiC nanocrystallites (white features in dark field) ranging in size from 1 to 15 nm embedded in an amorphous matrix. A TEM bright-field image showing the fiber, coatings and their interfaces (marked by arrows) is presented in Fig. 16. A crack is observed between the fiber and the p-B(Si)N coating and also a crack in the coatings perpendicular to the fiber surface that was not seen in p-BN/SiC coated Hi-Nicalon fibers. TEM energy dispersive X-ray spectra (EDXS) showing the chemical compositions of the fiber and the p-B(Si)N

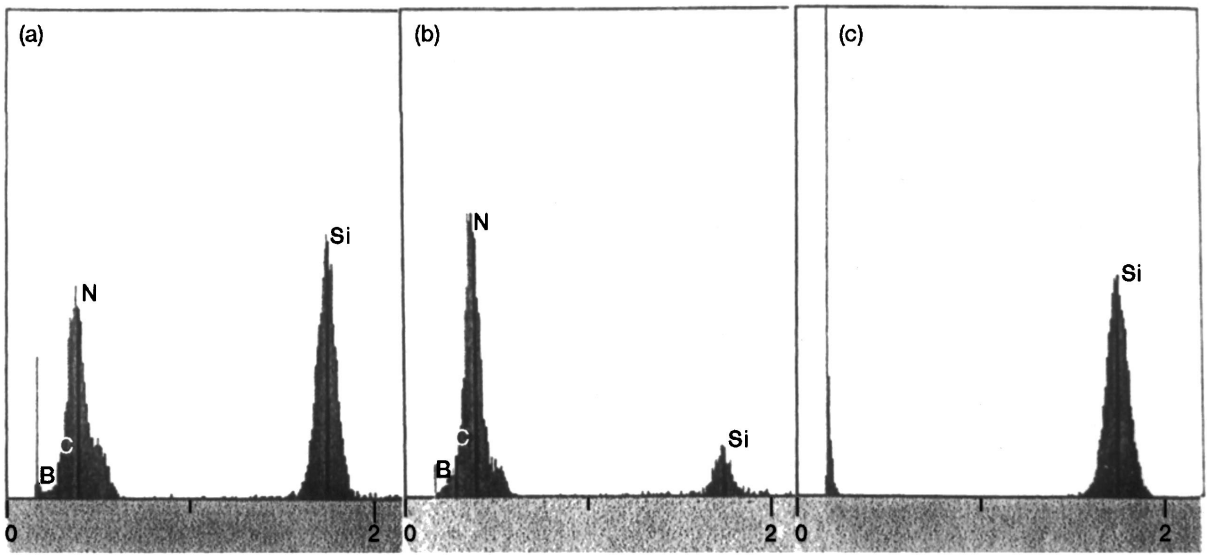


*Figure 11* Energy dispersive X-ray spectra collected from (a) fiber/p-BN interface, (b) middle of p-BN coating, and (c) SiC coating for p-BN/SiC coated Hi-Nicalon fiber.

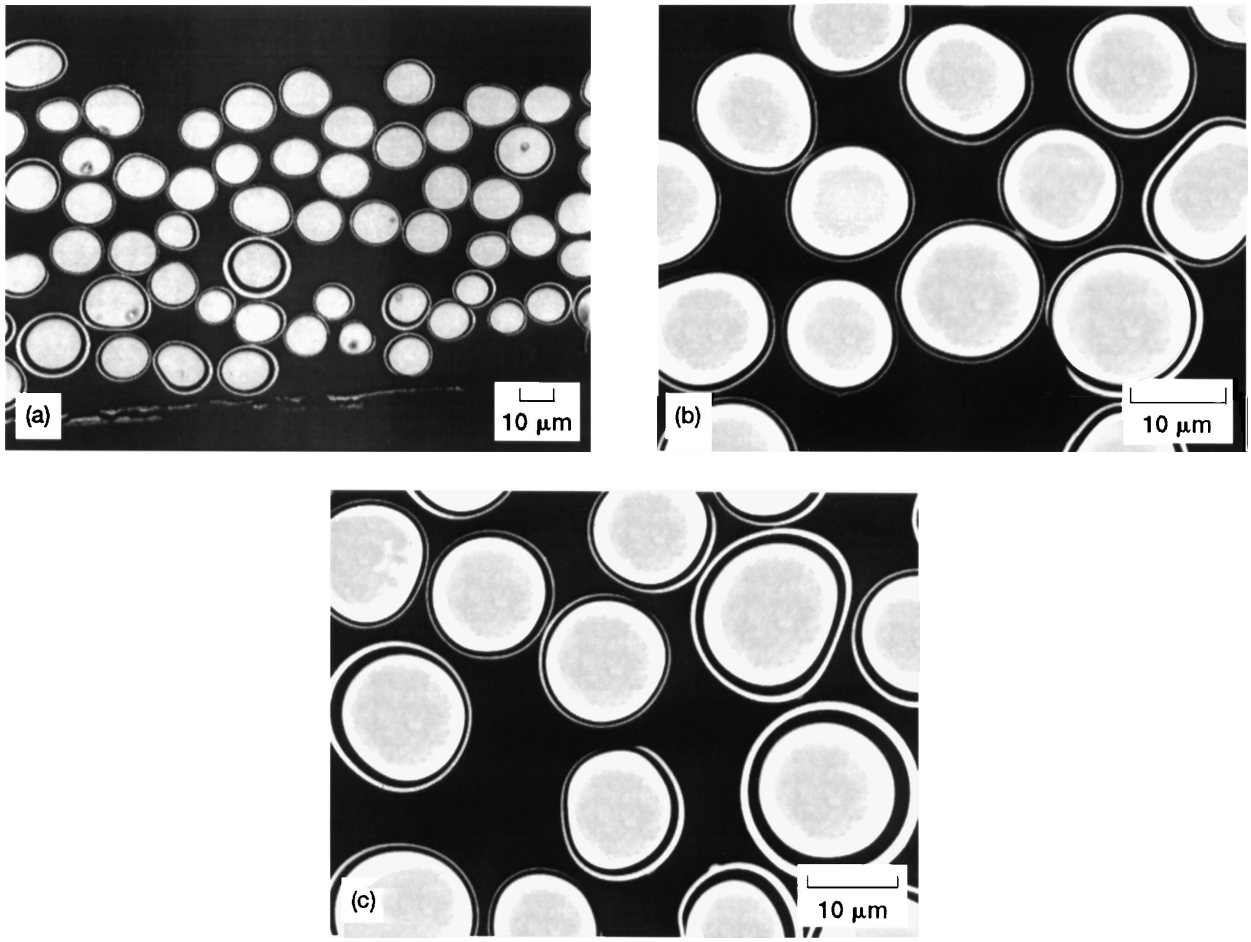


*Figure 12* SEM micrographs showing polished cross-sections of p-B(Si)N/SiC coated Hi-Nicalon fibers.

and SiC coatings are shown in Fig. 17. The Si is probably present as silicon nitride or some other compound within the p-BN coating. However, this needs to be further confirmed. It has been recently reported [4] that the p-B(Si)N coating, deposited under conditions similar to those used in the present study, was glassy and quite different from the p-BN coating which was turbostratic and showed considerable preferred orientation. Si and B were uniformly distributed.

## 4.2. Scanning Auger analysis

Elemental composition depth profiles, as obtained from scanning Auger analysis of as-received, but desized, Hi-Nicalon fibers and those having BN/SiC surface coatings are shown in Fig. 18a and b, respectively. Depth profiles of the p-BN/SiC and p-B(Si)N/SiC coated fibers are also presented in Fig. 18c and d, respectively. The elemental composition (at %) of the as-received fiber is ~42% Si and 56% C with C/Si atomic ratio

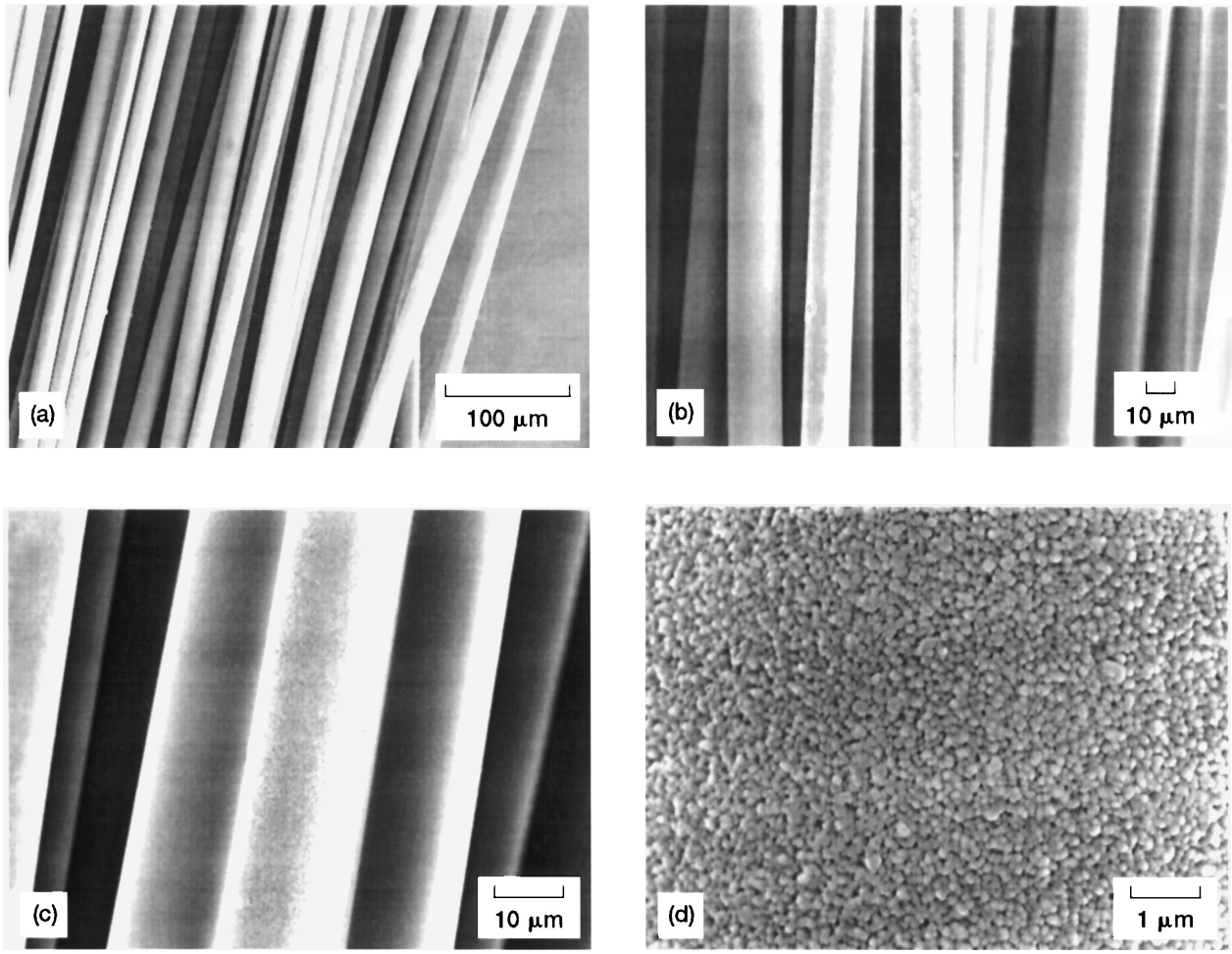


*Figure 13* SEM micrographs showing surfaces of p-B(Si)N/SiC coated Hi-Nicalon fibers.

of 1.33. A trace amount of oxygen is also detected. These results are in good agreement with the fiber composition supplied by the manufacturer (Table I). The Hi-Nicalon/BN/SiC fiber has ∼130 nm thick layer of Si-rich SiC followed by ∼500 nm thick layer of B-rich BN. However, the coating thicknesses were non-uniform from filament to filament as seen from the SEM micrographs in Figs 4 and 5. The fibers on the outside of a tow had thicker and more granular coatings than those on the inside. The BN coating is contaminated with oxygen and contains a high concentration of carbon. In fact, the concentration of carbon is larger than those of boron and nitrogen. The Hi-Nicalon/p-BN/SiC fiber has ∼300 nm thick layer of somewhat Si-rich SiC followed by ∼1500 nm thick layer of B-rich BN. A small amount of oxygen is also detected in the BN layer. However, no contamination with carbon was observed. The average thickness of p-BN and SiC coatings were 0.59 and 0.29 $\mu$m, respectively, as calculated from weight gains after CVD of each coating. The Hi-Nicalon/p-B(Si)N/SiC fiber shows a 0.8 $\mu$m thick layer of slightly Si-rich SiC followed by a 0.8 $\mu$m thick layer of boron-rich BN layer doped with 12 weight per cent of Si. No contamination with carbon or oxygen was observed. From weight gains after CVD of each coating, the average coating thicknesses of p-B(Si)N and SiC were calculated to be 0.6 and 0.3 $\mu$m, respectively by the vendor.

### 4.3. Tensile strength

The strength of ceramic fibers is determined by the statistical distribution of flaws in the material. The tensile strength of ceramic fibers is generally analyzed on the basis of the well known Weibull statistics [8]. An excellent review of the subject was provided by Van der Zwaag [9]. The Weibull modulus describes the distribution of strength in materials which fail at defects according to the weakest link statistics. The probability of survival of a material is given by the empirical equation:

$$P_s = 1 - P(\sigma) = \exp\left[-V\{(\sigma - \sigma_u)/\sigma_0\}^m\right] \quad (1)$$

where $P_s$ is the survival probability ($P(\sigma) = 1 - P_s$ is the failure probability) of an individual fiber at an applied stress of $\sigma$, $V$ is the fiber volume, $\sigma_u$ is the stress below which failure never occurs, $\sigma_0$ is the scale parameter, and $m$ is the shape or flaw dispersion parameter. For a given material, the Weibull modulus $m$ and $\sigma_0$ are constant. Assuming $\sigma_u = 0$ and uniform fiber diameter along the length, $L$, corresponding to the volume, $V$, Equation 1 can be rearranged as:

$$\ln\ln(1/P_s) = \ln\ln[1/(1 - P(\sigma))] = m\ln\sigma + \text{constant} \quad (2)$$

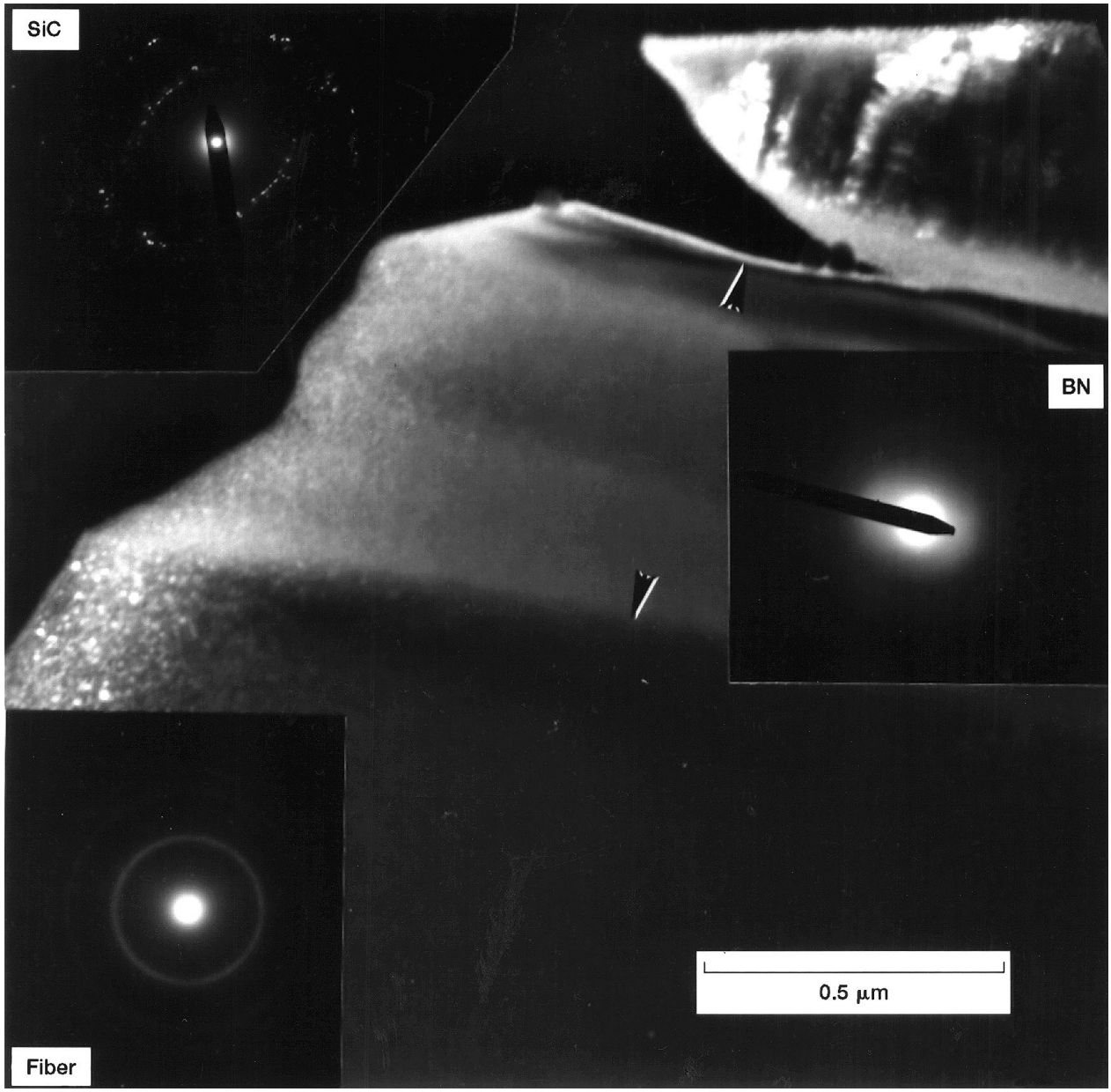


*Figure 14* TEM dark-field image showing microstructures of the fiber and the coatings and the interfaces between p-B(Si)N and SiC coatings and between p-B(Si)N coating and fiber for the p-B(Si)N/SiC coated Hi-Nicalon fiber. Also shown as insets are the selected area diffraction patterns from the fiber (marked fiber), p-B(Si)N coating (marked BN), and SiC coating (marked SiC).

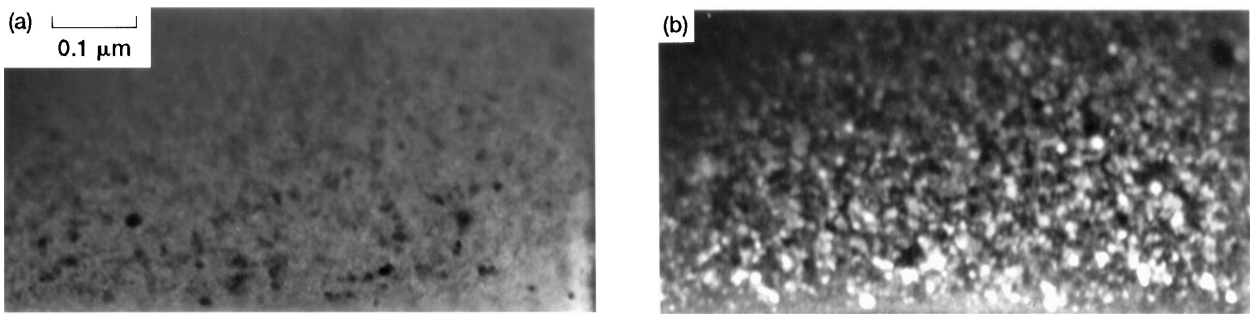


*Figure 15* A higher magnification pair of TEM bright-field (a) and dark-field (b) images showing fiber in the p-B(Si)N/SiC coated Hi-Nicalon fiber.

The experimental data are ranked in ascending order of strength values and the cumulative probability $P(\sigma_i)$ is assigned as

$$P(\sigma_i) = i/(1 + N) \quad (3)$$

where $i$ is the rank of the tested fiber in the ranked strength tabulation and $N$ is the total number of fibers tested. A least-squares linear regression analysis is then applied to a plot of $[\ln \ln 1/P_s]$ vs. $\ln(\sigma)$ whose slope is the Weibull modulus $m$.

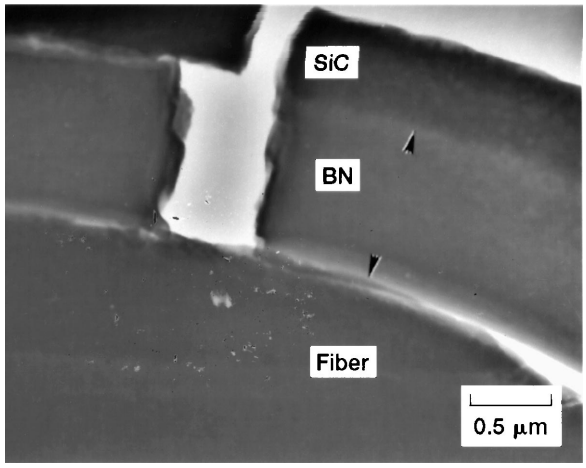


*Figure 16* TEM bright-field from p-B(Si)N/SiC coated Hi-Nicalon fiber shows cracking between the fiber and the p-B(Si)N coating and also a crack in the coatings normal to the fiber surface.

It has recently been reported [10, 11] that the strength and Weibull modulus of ceramic fibers obtained using measured and average values of fiber diameters were in good agreement. Therefore, an average fiber diameter of 13.5 $\mu$m, instead of the measured diameter for each filament, was used in calculating strength and Weibull modulus of fibers in the present study. The $\ln \ln(1/P_s)$ vs. $\ln \sigma$ Weibull probability plots for room temperature tensile strength of uncoated and BN/SiC coated Hi-Nicalon are presented in Fig. 19a and b and the values of Weibull parameters obtained from liner regression analysis are summarized in Table II. The tensile strength of as-received Hi-Nicalon fiber is $3.19 \pm 0.73$ GPa and the Weibull modulus, $m$, is 5.41. The manufacturer's information data sheet [1] reports a value of 2.8 GPa for the room temperature tensile strength of these fibers indicating a reasonably good agreement with the value obtained in the current study.

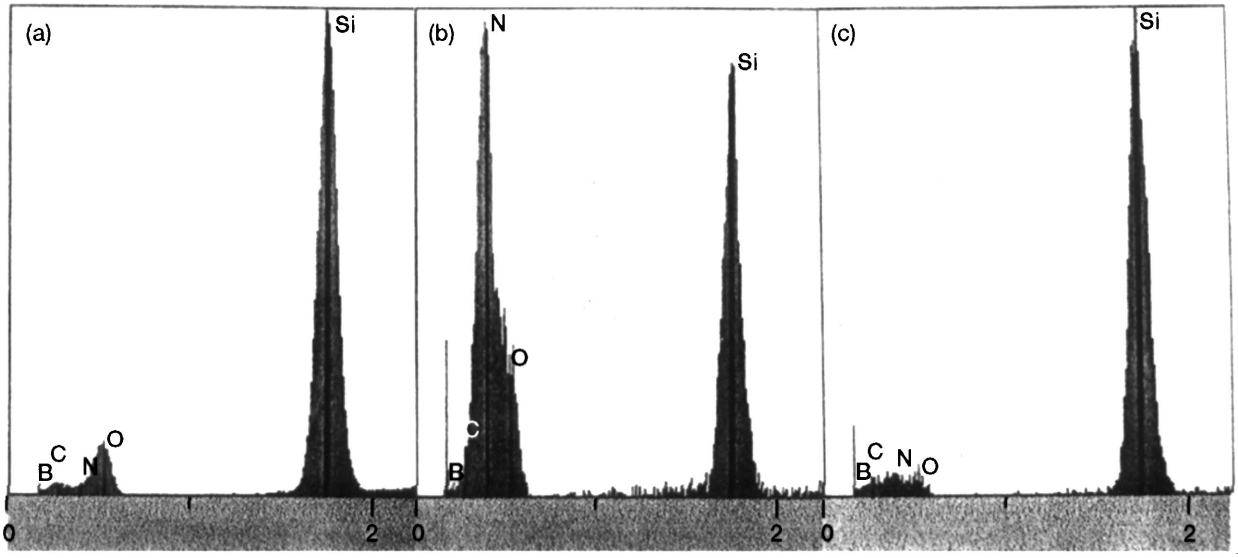


*Figure 17* Energy dispersive x-ray spectra showing chemical compositions of the (a) fiber, (b) p-B(Si)N coating, and (c) SiC coating in the p-B(Si)N/SiC coated Hi-Nicalon fiber.

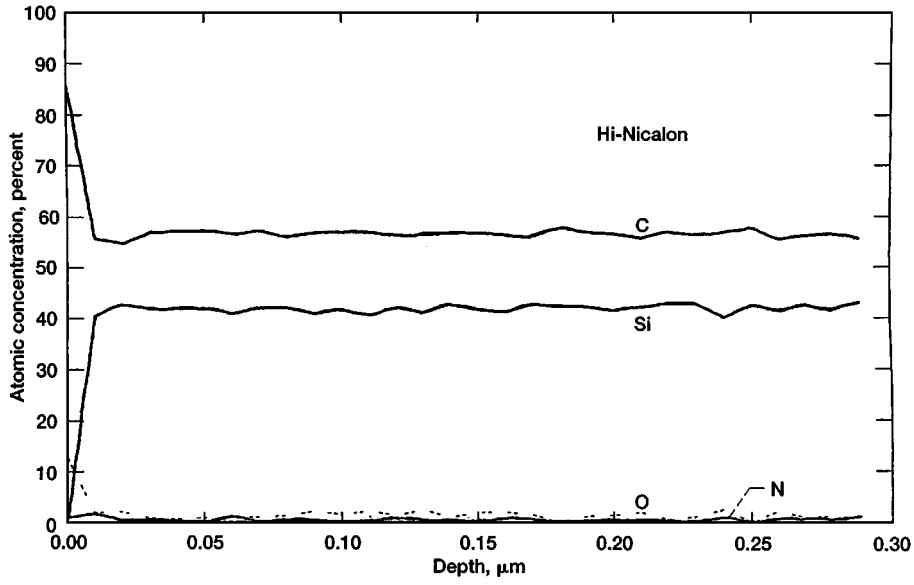


(a)

*Figure 18* Surface depth profiles of various elements obtained using scanning Auger microprobe for (a) Hi-Nicalon, (b) Hi-Nicalon/BN/SiC, (c) Hi-Nicalon/p-BN/SiC, and (d) Hi-Nicalon/p-B(Si)N/SiC fibers. (*Continued*).

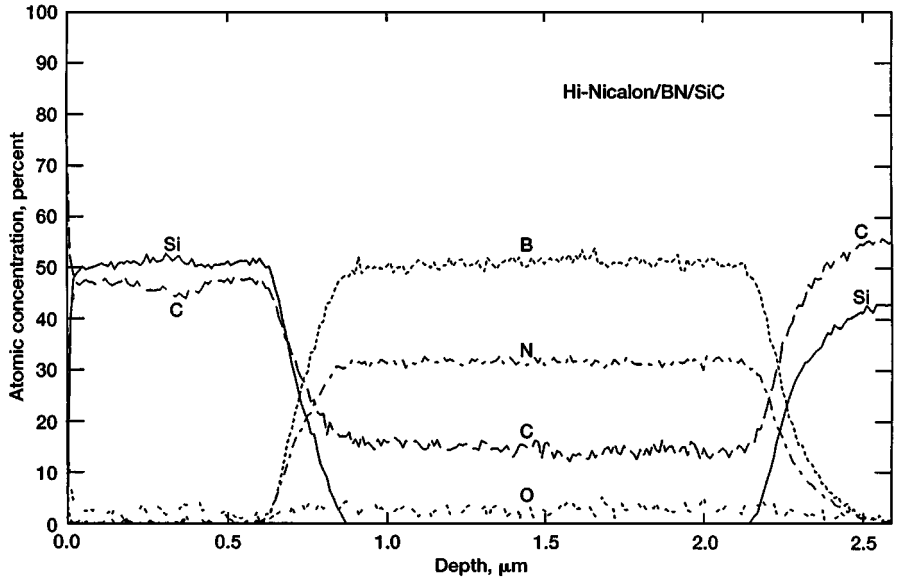


(b)

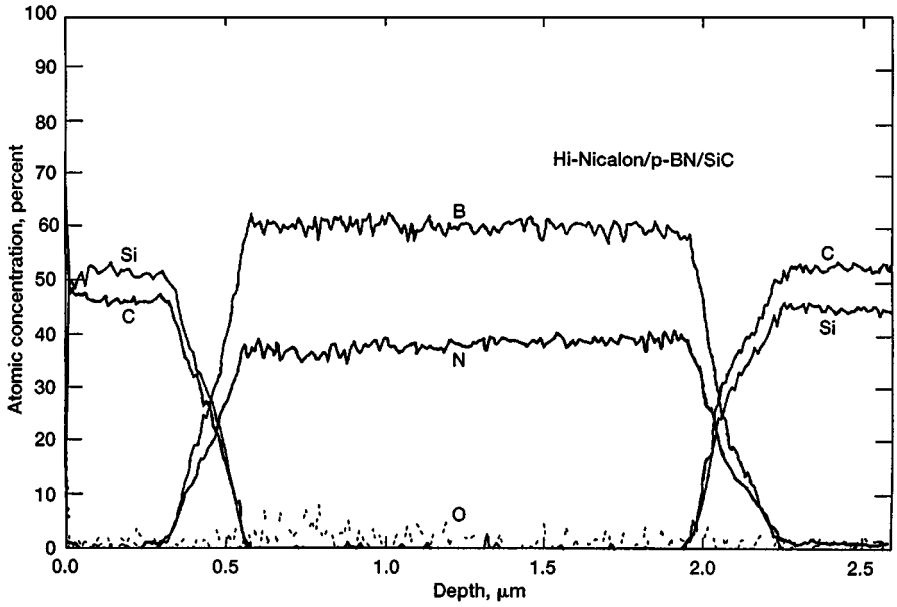


(c)

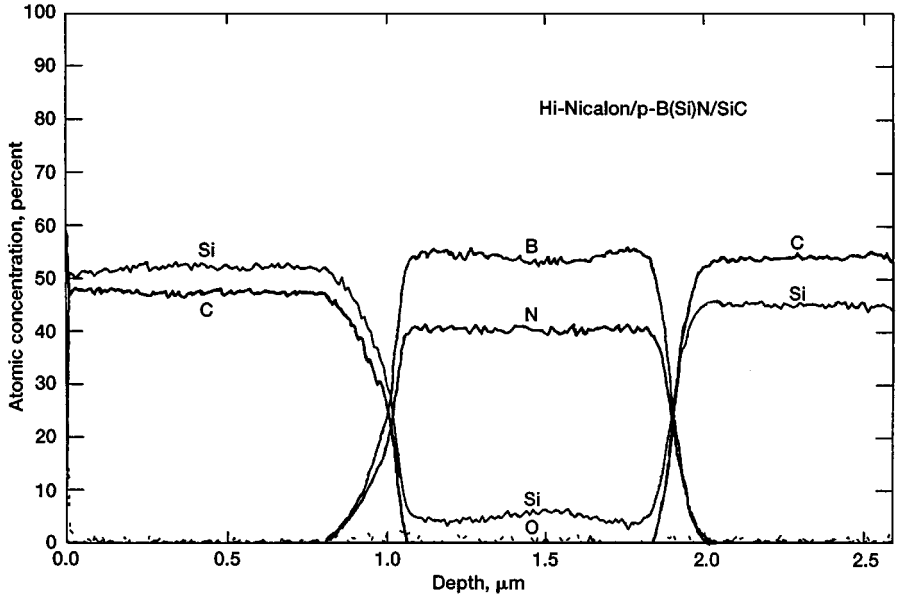


(d)

*Figure 18* (*Continued*).

TABLE II Weibull parameters for room temperature tensile strength of Hi-Nicalon fibers (gage length = 2.54 cm; crosshead speed = 1.261 mm/min)

| Fiber coating | Average strength (GPa) | Std. dev. (GPa) | Weibull modulus (m) |
|---|---|---|---|
| None (as-received, flame desized) | 3.19 | 0.73 | 5.41 |
| BN-SiC | 3.04 | 0.53 | 6.66 |
| p-BN/SiC | 2.80 | 0.42 | 7.96 |
| p-B(Si)N/SiC (12 wt % Si) | 2.17 | 0.52 | 4.99 |

An average fiber diameter of 13.5 $\mu$m used; 20 filaments tested for each fiber type.

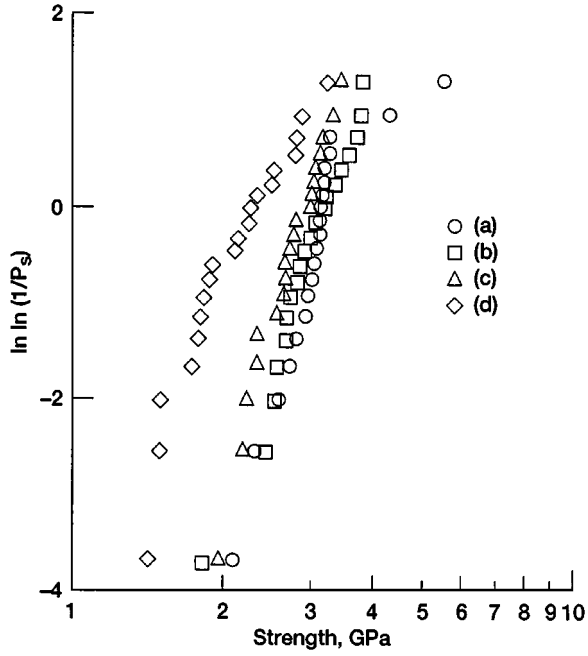


*Figure 19* Weibull probability plots for room temperature tensile strengths of Hi-Nicalon fibers: (a) uncoated, (b) BN/SiC coated, (c) p-BN/SiC coated, and (d) p-B(Si)N/SiC coated.

Weibull plots for the Hi-Nicalon fibers having p-BN/SiC and p-B(Si)N surface coatings are shown in Fig. 19c and d. Values of Weibull parameters obtained from linear regression analysis for these fibers are summarized in Table II. The p-BN/SiC coated and the p-B(Si)N/SiC coated Hi-Nicalon fibers show an average tensile strength of 2.80±0.42 GPa and 2.17±0.52 GPa with *m* values of 7.96 and 4.99, respectively. This indicates strength degradation of ∼10% and 35%, respectively during the application of these two coatings on the fibers by CVD. The small reduction in strength of p-BN/SiC coated fibers is probably due to the exposure of the fibers to 1400 °C for a short time during CVD coating. However, the large strength degradation for the p-B(Si)N/SiC coated fibers cannot be explained only due to exposure to high temperature. Probably the Si doping causes some chemical degradation of the fibers.

## 5. Summary

Tensile strengths of as-received Hi-Nicalon fibers and those having BN/SiC, p-BN/SiC, and p-B(Si)N/SiC surface coatings, deposited by chemical vapor deposition, were measured at room temperature. The Weibull statistical parameters were determined for each fiber. The average tensile strength of uncoated Hi-Nicalon was 3.19 ± 0.73 GPa with a Weibull modulus of 5.41. Strength of fibers coated with BN/SiC did not change. However, fibers with p-BN/SiC and p-B(Si)N/SiC surface coatings showed strength loss of ∼10% and 35%, respectively, compared with the as-received fibers.

The elemental compositions of the fibers and the coatings were analyzed using scanning Auger microprobe and energy dispersive X-ray spectroscopy. BN coating was contaminated with a large concentration of carbon and some oxygen. In contrast, p-BN, p-B(Si)N, and SiC coatings did not show any contamination. Microstructural analyses of the fibers and the coatings were done by scanning electron microscopy (SEM), transmission electron microscopy (TEM), and selected area electron diffraction. TEM analysis of the BN coating revealed four distinct layers with turbostratic structure. The p-BN layer was turbostratic and showed considerable preferred orientation. The p-B(Si)N was glassy and the silicon and boron were uniformly distributed. The silicon carbide coating consists of a columnar-like polycrystalline structure, the direction of the columns being along the growth direction. The p-B(Si)N/SiC coatings were more uniform, less defective and of better quality than the BN/SiC or the p-BN/SiC coatings.

## 6. Conclusions and future work

Tensile strength of Hi-Nicalon fibers is not effected by BN/SiC coating. However, p-BN/SiC and p-B(Si)N/SiC surface coatings degrade the fiber strength by ∼10 and 35%, respectively, possibly due to exposure to higher processing temperatures and interaction between the fiber and the coatings. Microstructure of the fiber remain unaffected during the coating process. Because of the higher thermo-oxidative stability of p-BN and p-B(Si)N, these coated Hi-Nicalon fibers of the current study are being used as reinforcement for fabrication of fiber-reinforced celsian matrix composites. The mechanical properties of these CMCs at elevated temperatures in oxidizing environments are being investigated. The data reported herein should aid in the interpretation of results from these additional studies.

## Acknowledgements

Thanks are due to Dan Gorican for fiber strength measurements, John Setlock for SEM, and Darwin Boyd for scanning Auger analysis.

## References

1. M. TAKEDA, J. SAKAMOTO, A. SAEKI and H. ICHIKAWA, *Ceram. Eng. Sci. Proc.* **16** (1995) 37.
2. N. P. BANSAL, *J. Amer. Ceram. Soc.* **80** (1997) 2407.
3. N. P. BANSAL and J. I. ELDRIDGE, *J. Mater. Res.* **13** (1998) 1530.
4. A. W. MOORE, H. SAYIR, S. C. FARMER and G. N. MORSCHER, *Ceram. Eng. Sci. Proc.* **16** (1995) 409.

5. N. P. BANSAL and R. M. DICKERSON, *Mater. Sci. Eng.* **A222** (1997) 149.
6. G. CHOLLON, R. PAILLER, R. NASLAIN and P. OLRY, *J. Mater. Sci.* **32** (1997) 1133.
7. T. SHIMOO, I. TSUKADA, M. NARISAWA, T. SEGUCHI and K. OKAMURA, *J. Ceram. Soc. Jpn.* **105** (1997) 559.
8. W. A. WEIBULL, *J. Appl. Mech. 18* (1951) 293.
9. S. VAN derZWAAG, *J. Testing Eval.* **17** (1989) 292.
10. N. P. BANSAL, Effects of HF Treatments on Tensile Strengths of Hi-Nicalon Fibers, NASA Technical Memorandum 206626, February 1998.
11. M. D. PETRY, T.-I. MAH and R. J. KERANS, *J. Amer. Ceram. Soc.* **80** (1997) 2741.

*Received 4 September*
*and accepted 18 September 1998*